PERGAMON

International Journal of Heat and Mass Transfer 43 (2000) 725–740

International Journal of HEAT and MASS TRANSFER

www.elsevier.com/locate/ijhmt

# Forced convection with slug flow and viscous dissipation in a rectangular duct

A. Barletta*, B. Pulvirenti

*Dipartimento di Ingegneria Energetica, Nucleare e del Controllo Ambientale (DIENCA), Università di Bologna, Viale Risorgimento 2, I-40136 Bologna, Italy*

Received 3 December 1998; received in revised form 17 May 1999

**Abstract**

Stationary forced convection in a rectangular duct is investigated in the case of slug flow by taking into account the effect of viscous dissipation. Axially-varying heat fluxes are prescribed on the four duct walls. Under the assumption that the axial heat conduction in the fluid is negligible, an analytical solution for the thermal entrance region is obtained by employing a superposition method. More precisely, the superposition method allows one to reduce the three-dimensional boundary value problem to a two-dimensional problem which is solved by the Laplace transform technique. The dimensionless temperature and the axially local Nusselt number are determined. Special attention is devoted to the eight fundamental boundary conditions of axially uniform wall heat fluxes and to the case of a peripherally uniform wall heat flux which undergoes an exponential axial variation. 

*Keywords:* Forced convection; Slug flow; Viscous dissipation; Analytical methods

## 1. Introduction

Several analyses of forced convection in rectangular ducts are available in the literature. The interest deserved to heat transfer in rectangular ducts as well as, in general, in noncircular ducts is primarily due to the applications in the field of compact heat exchangers. The most important investigations available in the literature on convection in rectangular ducts have been reviewed by Shah and London [1], Shah and Bhatti [2] and Hartnett and Kostic [3].

In the last decade, novel results in the field of forced convection in rectangular ducts have been obtained [4–10]. A generalized integral transform technique has been employed to analyze the thermal entrance region for laminar forced convection, in the case of a uniform wall temperature [4]. A numerical solution based on an implicit finite-difference method has been obtained in the hydrodynamically and thermally developed region for power-law fluids, in the case of uniform heat fluxes prescribed on the four walls of the duct [5]. By employing a superposition method together with an analytical solution in the case of slug flow in a duct with one uniformly heated wall and three adiabatic walls, Gao and Hartnett [6] obtained a general expression of the fully developed Nusselt number for eight different combinations of uniformly heated and adiabatic duct walls. A finite-difference scheme has

* Corresponding author. Tel.: +39-051-2093295; fax: +39-051-2093296.

*E-mail address:* antonio.barletta@mail.ing.unibo.it (A. Barletta).

0017-9310/00/$ - see front matter 
PII: S0017-9310(99)00187-8

**Nomenclature**

| | |
|---|---|
| $a_1$, $a_2$, $a_3$, $a_4$ | parameters such that $a_1 = a_2 = uL_y^2/\alpha$ and $a_3 = a_4 = uL_z^2/\alpha$ (m) |
| $a$ | dimensionless parameter employed in Eq. (55) |
| $b_1$, $b_2$, $b_3$, $b_4$ | dimensionless parameters employed in Eq. (44) |
| $Br$ | Brinkman number, $Br = \phi_0/q_0$ |
| $D_h$ | hydraulic diameter, $D_h = 2L_yL_z/(L_y + L_z)$ (m) |
| $f$ | dimensionless function defined by Eq. (53) |
| $f_1$, $f_2$, $f_3$, $f_4$ | dimensionless functions of $x$ employed in Eqs. (4) and (5) |
| $g_j(\xi)$ | dimensionless function of $\xi$, $g_j(\xi) = f_j(PeD_h\xi)$, for $j = 1, 2, 3, 4$ |
| $h_1$, $h_2$, $h_3$, $h_4$ | dimensionless functions employed in Eqs. (15) and (16) |
| $H$ | dimensionless function defined by Eq. (25) |
| $K(x, y, z)$ | arbitrary function employed in Eq. (32) |
| $k$ | thermal conductivity (W/m K) |
| $\mathscr{L}$ | Laplace transform operator |
| $L_y$ | long-side length of the duct section (m) |
| $L_z$ | short-side length of the duct section (m) |
| $L_{th}^*$ | dimensionless thermal entrance length |
| $M$ | dimensionless function defined in Eq. (58) |
| $n$ | positive integer |
| $Nu$ | Nusselt number defined by Eq. (38) |
| $p$ | dimensionless variable employed in Eqs. (58)–(63) |
| $Pe$ | Peclet number, $Pe = uD_h/\alpha$ |
| $q_0$ | reference wall heat flux (W/m$^2$) |
| $q_{w,m}$ | peripherally averaged wall heat flux (W/m$^2$) |
| $R_{Nu}$ | dimensionless parameter, $R_{Nu} = Nu/Nu_\infty$ |
| Res | residue of a complex function at a pole |
| $s$ | Laplace transform variable |
| $s_n$ | simple poles of function $\tilde{H}(s,\omega)$ |
| $t$ | dimensionless variable employed in Eqs. (17) and (18) |
| $T$ | temperature (K) |
| $T_0$ | inlet temperature (K) |
| $T_1$, $T_2$ | functions defined by Eqs. (6)–(10) (K) |
| $u$ | uniform fluid velocity (m/s) |
| $U$ | Heaviside's unit step function |
| $w_j(t)$ | dimensionless function of $t$, $w_j(t) = f_j(a_jt)$, for $j = 1, 2, 3, 4$ |
| $x$, $y$, $z$ | Cartesian coordinates (m) |
| $\alpha$ | thermal diffusivity (m$^2$/s) |
| $\beta$ | aspect ratio, $\beta = L_z/L_y$ |
| $\gamma$ | dimensionless parameter, $\gamma = 2\beta/(1 + \beta)$ |
| $\delta$ | Dirac's delta distribution |
| $\Delta\theta$ | dimensionless function, $\Delta\theta = \theta - \theta_b$ |
| $\zeta$ | dimensionless $z$-coordinate, $\zeta = z/L_y$ |
| $\eta$ | dimensionless $y$-coordinate, $\eta = y/L_y$ |
| $\theta$,$\theta_1$,$\theta_2$ | dimensionless temperatures defined by Eq. (28) |
| $\mu$ | dynamic viscosity (Pa s) |
| $\xi$ | dimensionless $x$-coordinate, $\xi = x/(D_hPe)$ |
| $\rho$ | mass density (kg/m$^3$) |
| $\Phi$ | viscous dissipation function (s$^{-2}$) |
| $\phi_0$ | parameter employed in Eq. (1) (W/m$^2$) |
| $\omega$ | dummy dimensionless variable |

*Superscripts*

| | |
|---|---|
| $\sim$ | Laplace transformed function |
| $'$ | dummy integration variable |

*Subscripts*

| | |
|---|---|
| b | bulk value |
| w, m | peripherally averaged wall quantity |
| $\infty$ | fully developed value |

been employed to investigate the thermally developing laminar forced convection for rectangular ducts with various aspect ratios and a peripherally and axially uniform wall heat flux [7]. With reference to the boundary conditions considered by Gao and Hartnett [6], Spiga and Morini [8,9] investigated the thermally developing region in the case of slug flow and evaluated the thermal entrance lengths for several values of the aspect ratio. The effect of viscous dissipation has been taken into account in the analysis of laminar forced convection in the hydrodynamically and thermally developed region for a rectangular duct with an

axially uniform wall heat flux and a peripherally uniform wall temperature [10].

Recently, a mathematical model has been proposed in order to investigate the effect of viscous dissipation for slug-flow forced convection in circular ducts [11]. Indeed, in the energy equation, the customary representation of the viscous heating power in terms of the spatial derivatives of the velocity field becomes singular in the case of slug flow. As is easily verified, for slug flow, the spatial derivatives of the velocity field are zero at every internal point of the duct and are infinite at the wall. As a consequence, the power generated per unit volume by viscous dissipation is distributed in the duct section as a Dirac's delta centered next to the duct wall. The model developed in Ref. [11] has been employed to evaluate the thermally developing temperature field and the local Nusselt number for slug flow forced convection in a circular duct both in the case of an arbitrary axially varying wall heat flux [12] and in the case of external convection with a fluid having an axially varying reference temperature [13].

The aim of the present paper is to apply the mathematical model employed in Refs. [11–13] to the case of a rectangular duct with slug flow and non-negligible viscous dissipation. Indeed, to the best of authors' knowledge, the effect of viscous dissipation has been always disregarded in previous analyses of slug-flow forced convection in rectangular ducts. In the following sections, an analytical solution of the energy balance equation is obtained for the thermal entrance region of a rectangular duct with arbitrary axially varying heat fluxes prescribed on the four duct walls. The solution is determined by employing the Laplace transform technique and a superposition method. A special attention is devoted to the case of uniform heat fluxes on the four walls and to the case of a peripherally uniform wall heat flux which undergoes an exponential axial variation.

## 2. Mathematical model

In this section, the boundary value problem for slug flow forced convection in a rectangular duct is formulated by taking into account the effect of viscous dissipation. Then, the equations are solved by means of a superposition method and of the Laplace transform technique. Finally, the solution is expressed in a dimensionless form.

Let us consider slug-flow forced convection within a rectangular duct. The duct geometry and coordinate system are represented in Fig. 1. The $x$-component of the fluid velocity is uniform within the duct, and is zero at the walls. The thermal properties of the fluid are assumed to be independent of temperature. Moreover, the axial heat conduction in the fluid is considered as negligible. Since the effect of viscosity is restricted to an infinitesimal layer adjacent to the duct walls, the power generated per unit volume by viscous dissipation can be expressed by a Dirac's delta distribution centered next to the four duct walls. Therefore, the viscous heating term in the energy balance equation can be expressed as

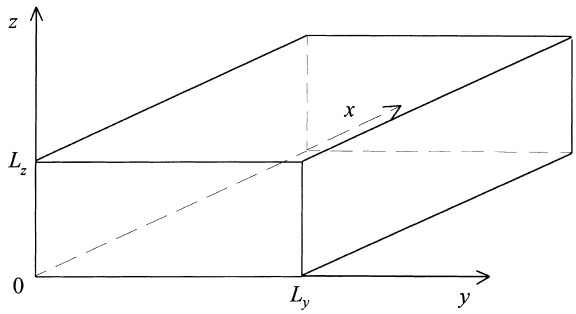


Fig. 1. Drawing of the duct and of the coordinate axes.

$$\mu\Phi(y,z) = \phi_0\big[\delta(y) + \delta\big(L_y - y\big) + \delta(z) + \delta(L_z - z)\big], \quad (1)$$

where $\delta$ is the one-dimensional Dirac's delta distribution and $2\phi_0(L_y + L_z)$ is the power dissipated by viscous heating per unit duct length. If the axial distributions of heat flux are prescribed on the four duct walls and the inlet temperature is uniform with a value $T_0$, the temperature field is determined by the boundary value problem

$$\frac{\partial^2 T}{\partial y^2} + \frac{\partial^2 T}{\partial z^2} = \frac{u}{\alpha}\frac{\partial T}{\partial x} - \frac{\phi_0}{k}\big[\delta(y) + \delta\big(L_y - y\big) + \delta(z) + \delta(L_z - z)\big], \quad (2)$$

$$T(0,y,z) = T_0, \quad (3)$$

$$k\frac{\partial T}{\partial y}\bigg|_{y=0} = -q_0 f_1(x), \quad k\frac{\partial T}{\partial y}\bigg|_{y=L_y} = q_0 f_2(x), \quad (4)$$

$$k\frac{\partial T}{\partial z}\bigg|_{z=0} = -q_0 f_3(x), \quad k\frac{\partial T}{\partial z}\bigg|_{z=L_z} = q_0 f_4(x), \quad (5)$$

where, for every $j = 1, 2, 3, 4$, function $f_j(x)$ is such that $f_j(0) = 0$.

By employing a superposition method, the solution of Eqs. (2)–(5) can be expressed as

$$T(x,y,z) = T_0 + T_1(x,y) + T_2(x,z), \quad (6)$$

where $T_1(x,y)$ is the solution of

$$\frac{\partial^2 T_1}{\partial y^2} = \frac{u}{\alpha}\frac{\partial T_1}{\partial x} - \frac{\phi_0}{k}\big[\delta(y) + \delta\big(L_y - y\big)\big], \tag{7}$$

$$T_1(0,y) = 0, \quad k\frac{\partial T_1}{\partial y}\bigg|_{y=0} = -q_0 f_1(x), \qquad k\frac{\partial T_1}{\partial y}\bigg|_{y=L_y} = q_0 f_2(x), \tag{8}$$

and $T_2(x,z)$ is the solution of

$$\frac{\partial^2 T_2}{\partial z^2} = \frac{u}{\alpha}\frac{\partial T_2}{\partial x} - \frac{\phi_0}{k}\big[\delta(z) + \delta(L_z - z)\big], \tag{9}$$

$$T_2(0,z) = 0, \quad k\frac{\partial T_2}{\partial z}\bigg|_{z=0} = -q_0 f_3(x), \qquad k\frac{\partial T_2}{\partial z}\bigg|_{z=L_z} = q_0 f_4(x). \tag{10}$$

In analogy with the method described in Refs. [11–13] for circular ducts, it is easily verified that an equivalent mathematical representation of Eqs. (7)–(10) is given by

$$\frac{\partial^2 T_1}{\partial y^2} = \frac{u}{\alpha}\frac{\partial T_1}{\partial x}, \tag{11}$$

$$T_1(0,y) = 0, \quad k\frac{\partial T_1}{\partial y}\bigg|_{y=0} = -q_0 f_1(x) - \phi_0, \qquad k\frac{\partial T_1}{\partial y}\bigg|_{y=L_y} = q_0 f_2(x) + \phi_0, \tag{12}$$

$$\frac{\partial^2 T_2}{\partial z^2} = \frac{u}{\alpha}\frac{\partial T_2}{\partial x}, \tag{13}$$

$$T_2(0,z) = 0, \quad k\frac{\partial T_2}{\partial z}\bigg|_{z=0} = -q_0 f_3(x) - \phi_0, \qquad k\frac{\partial T_2}{\partial z}\bigg|_{z=L_z} = q_0 f_4(x) + \phi_0. \tag{14}$$

Indeed, Eqs. (11)–(14) reveal that $T_1(x,y)$ and $T_2(x,z)$ can be expressed as

$$T_1(x,y) = \frac{q_0 L_y}{k}\left[h_2\left(\frac{x\alpha}{uL_y^2}, \frac{y}{L_y}\right) + h_1\left(\frac{x\alpha}{uL_y^2}, 1 - \frac{y}{L_y}\right)\right], \tag{15}$$

$$T_2(x,z) = \frac{q_0 L_z}{k}\left[h_4\left(\frac{x\alpha}{uL_z^2}, \frac{z}{L_z}\right) + h_3\left(\frac{x\alpha}{uL_z^2}, 1 - \frac{z}{L_z}\right)\right], \tag{16}$$

where, for every $j = 1, 2, 3, 4$, function $h_j(t,\omega)$ is defined as the solution of the differential problem

$$\frac{\partial^2 h_j}{\partial \omega^2} = \frac{\partial h_j}{\partial t}, \tag{17}$$

$$h_j(0,\omega) = 0, \quad \frac{\partial h_j}{\partial \omega}\bigg|_{\omega=0} = 0, \quad \frac{\partial h_j}{\partial \omega}\bigg|_{\omega=1} = w_j(t) + Br. \tag{18}$$

In Eq. (18), functions $w_j(t)$ are given by $w_j(t) = f_j(a_j t)$ for every $j = 1, 2, 3, 4$, where the coefficients $a_j$ are such that $a_1 = a_2 = uL_y^2/\alpha$ and $a_3 = a_4 = uL_z^2/\alpha$.

The solution of Eqs. (17) and (18) can be easily obtained by the Laplace transform method [14]. The transform of $h_j(t,\omega)$ is given by

$$\tilde{h}_j(s,\omega) = \int_0^\infty \mathrm{e}^{-st} h_j(t,\omega)\,\mathrm{d}t. \tag{19}$$

On account of the properties of Laplace transforms [14], Eqs. (17) and (18) yield

$$\frac{\partial^2 \tilde{h}_j}{\partial \omega^2} = s\tilde{h}_j, \tag{20}$$

$$\frac{\partial \tilde{h}_j}{\partial \omega}\bigg|_{\omega=0} = 0, \quad \frac{\partial \tilde{h}_j}{\partial \omega}\bigg|_{\omega=1} = \tilde{w}_j(s) + \frac{Br}{s}. \tag{21}$$

Eqs. (20) and (21) are easily solved, so that one obtains

$$\tilde{h}_j(s,\omega) = \frac{\cosh\big(\sqrt{s}\omega\big)}{s\sqrt{s}\,\sinh\big(\sqrt{s}\big)}\big[s\tilde{w}_j(s) + Br\big]. \tag{22}$$

On account of the convolution theorem for Laplace transforms [14], Eq. (22) yields

$$h_j(t,\omega) = BrH(t,\omega) + \int_0^t \frac{\mathrm{d}w_j(t')}{\mathrm{d}t'} H\big(t - t',\omega\big)\,\mathrm{d}t', \tag{23}$$

where $H(t,\omega)$ is defined as

$$H(t,\omega) = \mathscr{L}^{-1}\left\{\frac{\cosh\big(\sqrt{s}\omega\big)}{s\sqrt{s}\,\sinh\big(\sqrt{s}\big)}\right\}. \tag{24}$$

As is shown in the Appendix, the inverse Laplace transform which appears in the right-hand side of Eq. (24) is easily evaluated and $H(t,\omega)$ can be expressed as

$$H(t,\omega) = t + \frac{\omega^2}{2} - \frac{1}{6} - \frac{2}{\pi^2}\sum_{n=1}^{\infty}\frac{(-1)^n}{n^2}\exp\big(-n^2\pi^2 t\big)\cos(n\pi\omega). \tag{25}$$

Therefore, on account of Eqs. (15), (16) and (23), the functions $T_1(x,y)$ and $T_2(x,z)$ can be expressed as

$$T_1(x,y)=\frac{q_0L_y}{k}\left\{Br\left[H\left(\frac{x\alpha}{uL_y^2},\frac{y}{L_y}\right)+H\left(\frac{x\alpha}{uL_y^2},1-\frac{y}{L_y}\right)\right]+\int_0^x\frac{\mathrm{d}f_2(x')}{\mathrm{d}x'}H\left(\frac{\alpha}{uL_y^2}(x-x'),\frac{y}{L_y}\right)\mathrm{d}x'+\int_0^x\frac{\mathrm{d}f_1(x')}{\mathrm{d}x'}H\left(\frac{\alpha}{uL_y^2}(x-x'),1-\frac{y}{L_y}\right)\mathrm{d}x'\right\},\tag{26}$$

$$T_2(x,z)=\frac{q_0L_z}{k}\left\{Br\left[H\left(\frac{x\alpha}{uL_z^2},\frac{z}{L_z}\right)+H\left(\frac{x\alpha}{uL_z^2},1-\frac{z}{L_z}\right)\right]+\int_0^x\frac{\mathrm{d}f_4(x')}{\mathrm{d}x'}H\left(\frac{\alpha}{uL_z^2}(x-x'),\frac{z}{L_z}\right)\mathrm{d}x'+\int_0^x\frac{\mathrm{d}f_3(x')}{\mathrm{d}x'}H\left(\frac{\alpha}{uL_z^2}(x-x'),1-\frac{z}{L_z}\right)\mathrm{d}x'\right\},\tag{27}$$

By defining the dimensionless quantities

$$\xi=\frac{x}{D_\mathrm{h}Pe},\quad \eta=\frac{y}{L_y},\quad \zeta=\frac{z}{L_y},\quad \theta=k\frac{T-T_0}{q_0D_\mathrm{h}},\quad \theta_1=k\frac{T_1}{q_0D_\mathrm{h}},\quad \theta_2=k\frac{T_2}{q_0D_\mathrm{h}},\quad Pe=\frac{uD_\mathrm{h}}{\alpha},\quad \beta=\frac{L_z}{L_y},\quad \gamma=\frac{2\beta}{1+\beta},\tag{28}$$

Eqs. (6), (26) and (27) can be rewritten as

$$\theta(\xi,\eta,\zeta)=\theta_1(\xi,\eta)+\theta_2(\xi,\zeta),\tag{29}$$

$$\theta_1(\xi,\eta)=\frac{Br}{\gamma}\left[H\left(\xi\gamma^2,\eta\right)+H\left(\xi\gamma^2,1-\eta\right)\right]+\frac{1}{\gamma}\int_0^\xi\frac{\mathrm{d}g_1(\xi')}{\mathrm{d}\xi'}H\left(\gamma^2(\xi-\xi'),1-\eta\right)\mathrm{d}\xi'+\frac{1}{\gamma}\int_0^\xi\frac{\mathrm{d}g_2(\xi')}{\mathrm{d}\xi'}H\left(\gamma^2(\xi-\xi'),\eta\right)\mathrm{d}\xi',\tag{30}$$

$$\theta_2(\xi,\zeta)=\frac{Br\beta}{\gamma}\left[H\left(\frac{\xi\gamma^2}{\beta^2},\frac{\zeta}{\beta}\right)+H\left(\frac{\xi\gamma^2}{\beta^2},1-\frac{\zeta}{\beta}\right)\right]+\frac{\beta}{\gamma}\int_0^\xi\frac{\mathrm{d}g_3(\xi')}{\mathrm{d}\xi'}H\left(\frac{\gamma^2}{\beta^2}(\xi-\xi'),1-\frac{\zeta}{\beta}\right)\mathrm{d}\xi'+\frac{\beta}{\gamma}\int_0^\xi\frac{\mathrm{d}g_4(\xi')}{\mathrm{d}\xi'}H\left(\frac{\gamma^2}{\beta^2}(\xi-\xi'),\frac{\zeta}{\beta}\right)\mathrm{d}\xi',\tag{31}$$

where $g_j(\xi)=f_j(PeD_\mathrm{h}\xi)$, for every $j=1, 2, 3, 4$.

## 3. Bulk temperature and Nusselt number

In this section, expressions of the bulk temperature and of the local Nusselt number are obtained.

For slug flow, the bulk value of an arbitrary function $K(x,y,z)$ is given by

$$K_\mathrm{b}(x)=\frac{1}{L_yL_z}\int_0^{L_z}\int_0^{L_y}K(x,y,z)\,\mathrm{d}y\,\mathrm{d}z.\tag{32}$$

On account of Eqs. (6) and (32), the bulk temperature can be expressed as

$$T_\mathrm{b}(x)=T_0+T_{1\mathrm{b}}(x)+T_{2\mathrm{b}}(x).\tag{33}$$

Moreover, as a consequence of Eqs. (12), (14) and (32), if one integrates both sides of Eq. (11) with respect to $y$ in the interval $[0, L_y]$ and if one integrates both sides of Eq. (13) with respect to $z$ in the interval $[0, L_z]$, one is led to the following expressions:

$$T_{1\mathrm{b}}(x)=\frac{2\alpha\phi_0}{kuL_y}x+\frac{\alpha q_0}{kuL_y}\int_0^x\left[f_1(x')+f_2(x')\right]\mathrm{d}x',\tag{34}$$

$$T_{2\mathrm{b}}(x)=\frac{2\alpha\phi_0}{kuL_z}x+\frac{\alpha q_0}{kuL_z}\int_0^x\left[f_3(x')+f_4(x')\right]\mathrm{d}x',\tag{35}$$

Eqs. (34) and (35) can be written in a dimensionless form by employing Eq. (28), namely

$$\theta_{1\mathrm{b}}(\xi)=2\gamma Br\xi+\gamma\int_0^\xi\left[g_1(\xi')+g_2(\xi')\right]\mathrm{d}\xi',\tag{36}$$

$$\theta_{2\mathrm{b}}(\xi)=\frac{2\gamma Br}{\beta}\xi+\frac{\gamma}{\beta}\int_0^\xi\left[g_3(\xi')+g_4(\xi')\right]\mathrm{d}\xi'.\tag{37}$$

The peripherally uniform and axially local Nusselt number $Nu$ is defined as [1,15]

$$Nu=\frac{D_\mathrm{h}}{k}\frac{q_{\mathrm{w,m}}(x)}{T_{\mathrm{w,m}}(x)-T_\mathrm{b}(x)},\tag{38}$$

where $q_{\mathrm{w,m}}(x)$ is the peripherally averaged wall heat flux, which, on account of Eqs. (4) and (5), is

expressed as

$$q_{w,m}(x) = \frac{q_0 L_z\big[f_1(x)+f_2(x)\big] + q_0 L_y\big[f_3(x)+f_4(x)\big]}{2\big(L_y+L_z\big)}, \tag{39}$$

while $T_{w,m}(x)$ is the peripherally averaged wall temperature given by

$$T_{w,m}(x) = \frac{1}{2\big(L_y+L_z\big)}\left\{\int_0^{L_y}\big[T(x,y,0)+T(x,y,L_z)\big]\,dy + \int_0^{L_z}\big[T(x,0,z)+T\big(x,L_y,z\big)\big]\,dz\right\}. \tag{40}$$

By employing Eqs. (6) and (33), Eq. (40) can be rewritten as

$$T_{w,m}(x) = T_0 + \frac{L_y}{2\big(L_y+L_z\big)}\big[2T_{1b}(x)+T_2(x,0) + T_2(x,L_z)\big] + \frac{L_z}{2\big(L_y+L_z\big)}\big[2T_{2b}(x) + T_1(x,0)+T_1\big(x,L_y\big)\big]. \tag{41}$$

Then, Eq. (41) can be expressed in terms of the dimensionless quantities defined in Eq. (28) as follows:

$$\theta_{w,m}(\xi) = \frac{\gamma}{4\beta}\big[2\theta_{1b}(\xi)+\theta_2(\xi,0)+\theta_2(\xi,\beta)\big] + \frac{\gamma}{4}\big[2\theta_{2b}(\xi)+\theta_1(\xi,0)+\theta_1(\xi,1)\big]. \tag{42}$$

Moreover, Eqs. (28), (38) and (39) yield

$$Nu = \frac{\beta\big[g_1(\xi)+g_2(\xi)\big]+g_3(\xi)+g_4(\xi)}{2(1+\beta)\big[\theta_{w,m}(\xi)-\theta_b(\xi)\big]}. \tag{43}$$

Eqs. (30), (31), (36), (37) and (42) allow one to evaluate the axial distribution of $Nu$ for every choice of the functions $g_1(\xi)$, $g_2(\xi)$, $g_3(\xi)$ and $g_4(\xi)$.

## 4. Uniform heat fluxes on the duct walls

In this section, the expressions of dimensionless temperature and of the local Nusselt number obtained in Sections 2 and 3 are employed in the case of uniform heat fluxes on the four duct walls.

Let us assume that the functions $g_1(\xi)$, $g_2(\xi)$, $g_3(\xi)$ and $g_4(\xi)$ are given by

$$g_1(\xi) = b_1 U(\xi), \quad g_2(\xi) = b_2 U(\xi), \quad g_3(\xi) = b_3 U(\xi), \quad g_4(\xi) = b_4 U(\xi), \tag{44}$$

where $b_1$, $b_2$, $b_3$ and $b_4$ are arbitrary real numbers.

On account of Eq. (44), Eqs. (30) and (31) yield

$$\theta_1(\xi,\eta) = \frac{Br+b_2}{\gamma}H\big(\xi\gamma^2,\eta\big) + \frac{Br+b_1}{\gamma}H\big(\xi\gamma^2,1-\eta\big), \tag{45}$$

$$\theta_2(\xi,\zeta) = \frac{(Br+b_4)\beta}{\gamma}H\left(\frac{\xi\gamma^2}{\beta^2},\frac{\zeta}{\beta}\right) + \frac{(Br+b_3)\beta}{\gamma}H\left(\frac{\xi\gamma^2}{\beta^2},1-\frac{\zeta}{\beta}\right), \tag{46}$$

while Eqs. (36) and (37) can be rewritten as

$$\theta_{1b}(\xi) = \gamma(2Br+b_1+b_2)\xi, \quad \theta_{2b}(\xi) = \frac{\gamma}{\beta}(2Br+b_3+b_4)\xi. \tag{47}$$

As a consequence of Eqs. (43) and (44), for $\xi > 0$, the local Nusselt number is given by

$$Nu = \frac{\beta(b_1+b_2)+b_3+b_4}{2(1+\beta)\big[\theta_{w,m}(\xi)-\theta_b(\xi)\big]}. \tag{48}$$

Eqs. (25), (42) and (47), imply that the difference $\theta_{w,m}(\xi)-\theta_b(\xi)$ can be expressed as

$$\theta_{w,m}(\xi)-\theta_b(\xi) = \frac{1}{24}(4Br+b_1+b_2+b_3+b_4) - \frac{2Br+b_1+b_2}{4\pi^2}\sum_{n=1}^{\infty}\frac{1}{n^2}\exp\big(-4n^2\pi^2\gamma^2\xi\big) - \frac{2Br+b_3+b_4}{4\pi^2}\sum_{n=1}^{\infty}\frac{1}{n^2}\exp\left(-4n^2\pi^2\frac{\gamma^2}{\beta^2}\xi\right). \tag{49}$$

Therefore, Eqs. (48) and (49) predict that a fully developed value of the local Nusselt number is reached in the limit $\xi\to\infty$. The fully developed value is given by

$$Nu_\infty = \frac{12\big[\beta(b_1+b_2)+b_3+b_4\big]}{(1+\beta)(4Br+b_1+b_2+b_3+b_4)}. \tag{50}$$

The eight boundary conditions examined by Gao and Hartnett [6] and denoted by 4, 3L, 3S, 2L, 2S, 2C, 1L and 1S are special cases of Eq. (44). The values of $b_1$, $b_2$, $b_3$ and $b_4$ which define these eight cases are reported in Table 1. By employing Eq. (50) and the Gao–Hartnett boundary conditions, the fully developed Nusselt numbers for the cases 4, 3L, 3S, 2L, 2S, 2C, 1L and 1S are easily obtained and are reported in

Table 1
Values of $b_1$, $b_2$, $b_3$ and $b_4$ for the boundary conditions 4, 3L, 3S, 2L, 2S, 2C, 1L and 1S

| | $b_1$ | $b_2$ | $b_3$ | $b_4$ |
|---|---|---|---|---|
| 4 | 1 | 1 | 1 | 1 |
| 3L | 1 | 0 | 1 | 1 |
| 3S | 1 | 1 | 1 | 0 |
| 2L | 0 | 0 | 1 | 1 |
| 2S | 1 | 1 | 0 | 0 |
| 2C | 1 | 0 | 0 | 1 |
| 1L | 0 | 0 | 0 | 1 |
| 1S | 1 | 0 | 0 | 0 |

Table 2. On account of Table 2, one can conclude that the fully developed values of $Nu$ for $Br = 0$ are different from those obtained in Ref. [6], except in the cases 4, 2L and 2S. The reason relies in the different definitions of $Nu$ adopted in the present paper and in the paper by Gao and Hartnett [6]. The definition of $Nu$ employed in Ref. [6] is similar but not coincident with the definition of axially local Nusselt number adopted in the present paper and expressed by Eq. (38). Indeed, Gao and Hartnett [6] consider the quantities $q_{w,m}(x)$ and $T_{w,m}(x)$ as average values on the non-adiabatic walls and not on the whole periphery. For instance,

Table 2
Values of $Nu_\infty$ for the boundary conditions 4, 3L, 3S, 2L, 2S, 2C, 1L and 1S

| | $Nu_\infty$ |
|---|---|
| 4 | $\dfrac{6}{Br+1}$ |
| 3L | $\dfrac{12(2+\beta)}{(1+\beta)(4Br+3)}$ |
| 3S | $\dfrac{12(1+2\beta)}{(1+\beta)(4Br+3)}$ |
| 2L | $\dfrac{12}{(1+\beta)(2Br+1)}$ |
| 2S | $\dfrac{12\beta}{(1+\beta)(2Br+1)}$ |
| 2C | $\dfrac{6}{2Br+1}$ |
| 1L | $\dfrac{12}{(1+\beta)(4Br+1)}$ |
| 1S | $\dfrac{12\beta}{(1+\beta)(4Br+1)}$ |

according to Gao–Hartnett's definition, $q_{w,m}(x)$ coincides with $q_0$ in all the eight cases 4, 3L, 3S, 2L, 2S, 2C, 1L and 1S. Therefore, the Nusselt number defined by Eq. (38) is equal to that defined in Ref. [6] when all the duct walls are heated, as in case 4.

Table 2 reveals that $Nu_\infty$ depends on $\beta$ and on $Br$, except in the cases 4 and 2C where $Nu_\infty$ depends only on $Br$. This table shows that, for a given boundary condition and for a given aspect ratio, the effect of viscous dissipation tends to lower the value of $Nu_\infty$ if the fluid is heated ($Br > 0$), while it increases $Nu_\infty$ if the fluid is cooled ($Br < 0$). This behavior has been already pointed out with reference to circular ducts with a prescribed heat flux [11,12]. In the limit $\beta \to 0$, the rectangular duct becomes a parallel-plate channel either with a prescribed uniform heat flux on both walls (4, 3L, 2L), or with an adiabatic wall and with a prescribed uniform heat flux on the other wall (3S, 2C, 1L), or with two adiabatic walls (2S, 1S). In this limit, $Nu_\infty$ tends to zero both in case 2S and in case 1S. On the contrary, in the three cases 4, 3L, 2L, three different limits of $Nu_\infty$ are found for $\beta \to 0$. Moreover, also in the three cases 3S, 2C, 1L, three different limits of $Nu_\infty$ are found for $\beta \to 0$. This unexpected feature of the limit for $\beta \to 0$ is present also in the expressions of $Nu_\infty$ found by Gao and Hartnett [6], as it has been pointed out by Spiga and Morini [9]. Indeed, the limit for $\beta \to 0$ of the expressions of $Nu_\infty$ reported in Table 2 is not legitimate for the following reason. The expression of $Nu_\infty$ given by Eq. (50) has been obtained by considering the infinite sums present in Eq. (49) as negligible in the limit $\xi \to \infty$. However, if one lets $\beta \to 0$ in Eq. (49) the first infinite sum becomes independent of $\xi$ and, as is easily verified, equals $\pi^2/6$. Therefore, if $\beta \to 0$, the fully developed expression of $\theta_{w,m} - \theta_b$ is not $(4Br + b_1 + b_2 + b_3 + b_4)/24$, but $(2Br + b_3 + b_4)/24$. As a consequence, the limit for $\beta \to 0$ of the right-hand side of Eq. (50) is physically meaningless and the correct $Nu_\infty$ for a parallel-plate channel is given by

$$Nu_\infty = \frac{12(b_3 + b_4)}{2Br + b_3 + b_4}. \tag{51}$$

Obviously, the right-hand side of Eq. (51) is independent of the values of $b_1$ and $b_2$.

The dimensionless thermal entrance length $L^*_{th}$ is defined as the value of $\xi$ required to achieve a local Nusselt number $Nu$ equal to $1.05Nu_\infty$ [1]. As a consequence, the behavior of $L^*_{th}$ is easily investigated by evaluating the ratio $R_{Nu} = Nu/Nu_\infty$. On account of Eqs. (48)–(50), $1/R_{Nu}$ can be expressed as

Table 3
Values of $L^*_{th}$ for the boundary conditions 4, 3L, 3S, 2L, 2S, 2C, 1L and 1S, in the case $Br = 0$

| $\beta$ | 4 | 3L | 3S | 2L | 2S | 2C | 1L | 1S |
|---|---|---|---|---|---|---|---|---|
| 1 | 0.0645 | 0.0645 | 0.0645 | 0.0645 | 0.0645 | 0.0645 | 0.0645 | 0.0645 |
| 0.9 | 0.0653 | 0.0629 | 0.0675 | 0.0582 | 0.0719 | 0.0653 | 0.0582 | 0.0719 |
| 0.8 | 0.0679 | 0.0628 | 0.0728 | 0.0523 | 0.0817 | 0.0679 | 0.0523 | 0.0817 |
| 0.7 | 0.0738 | 0.0648 | 0.0819 | 0.0466 | 0.0951 | 0.0738 | 0.0466 | 0.0951 |
| 0.6 | 0.0851 | 0.0705 | 0.0969 | 0.0413 | 0.1147 | 0.0851 | 0.0413 | 0.1147 |
| 0.5 | 0.1059 | 0.0841 | 0.1221 | 0.0363 | 0.1452 | 0.1059 | 0.0363 | 0.1452 |
| 0.4 | 0.1439 | 0.1127 | 0.1661 | 0.0316 | 0.1976 | 0.1439 | 0.0316 | 0.1976 |
| 0.3 | 0.2205 | 0.1726 | 0.2547 | 0.0273 | 0.3029 | 0.2205 | 0.0273 | 0.3029 |
| 0.2 | 0.4228 | 0.3309 | 0.4883 | 0.0232 | 0.5806 | 0.4228 | 0.0232 | 0.5806 |
| 0.1 | 1.4211 | 1.1121 | 1.6411 | 0.0195 | 1.9516 | 1.4211 | 0.0195 | 1.9516 |
| 0 | 0.0161 | 0.0161 | 0.0161 | 0.0161 | – | 0.0161 | 0.0161 | – |

$$\frac{1}{R_{Nu}} = 1 - \frac{2Br + b_1 + b_2}{4Br + b_1 + b_2 + b_3 + b_4} f\left(\gamma^2 \xi\right) - \frac{2Br + b_3 + b_4}{4Br + b_1 + b_2 + b_3 + b_4} f\left(\frac{\gamma^2}{\beta^2}\xi\right), \tag{52}$$

where function $f$ is defined as

$$f(\omega) = \frac{6}{\pi^2} \sum_{n=1}^{\infty} \frac{\exp(-4\pi^2 n^2 \omega)}{n^2}. \tag{53}$$

On account of Eqs. (48), (49) and (51), in the limit $\beta \to 0, 1/R_{Nu}$ is given by

$$\frac{1}{R_{Nu}} = 1 - f(4\xi). \tag{54}$$

The following results are easily inferred by employing Eq. (52) and Table 1. The values of $R_{Nu}$ and $L^*_{th}$ in case 4 coincide with those in case 2C and are independent of $Br$. If $Br \to \infty$ and for every value of $\beta$, the same values of $R_{Nu}$ and $L^*_{th}$ are obtained in the eight cases 4, 3L, 3S, 2L, 2S, 2C, 1L and 1S. This is not surprising since, when $Br \to \infty$, all the eight boundary conditions degenerate to a single one, i.e., that of adiabatic walls. If $\beta = 1$, $R_{Nu}$ and $L^*_{th}$ are independent of $Br$ and of the parameters $b_1$, $b_2$, $b_3$ and $b_4$. The latter result is quite interesting and can be restated as follows. For a square duct, the same ratio $Nu/Nu_\infty$ and, as a consequence, the same dimensionless thermal entrance length are obtained for all the eight boundary conditions 4, 3L, 3S, 2L, 2S, 2C, 1L and 1S. This property does not hold if Gao–Hartnett's definition of local Nusselt number is employed, as is easily verified by examining the values of $L^*_{th}$ for $Br = 0$ reported by Spiga and Morini [8].

Eq. (54) shows that, in the limit $\beta \to 0$, $R_{Nu}$ and $L^*_{th}$ are independent of $Br$ and of the parameters $b_1$, $b_2$, $b_3$ and $b_4$. Although, in this limit, the conclusion that the parameters $b_1$ and $b_2$ do not influence $R_{Nu}$ and $L^*_{th}$ is obvious, a less obvious result is that $R_{Nu}$ and $L^*_{th}$ are independent of $Br$, $b_3$ and $b_4$.

In Table 3, the values of $L^*_{th}$ for $Br = 0$ are obtained

Table 4
Values of $L^*_{th}$ for the boundary condition 2L and for some values of $Br$

| $\beta$ | $Br = 0.1$ | $Br = 0.2$ | $Br = 0.4$ | $Br = 0.6$ | $Br = 0.8$ | $Br = 1$ | $Br = 2$ | $Br = 10$ |
|---|---|---|---|---|---|---|---|---|
| 1 | 0.0645 | 0.0645 | 0.0645 | 0.0645 | 0.0645 | 0.0645 | 0.0645 | 0.0645 |
| 0.9 | 0.0594 | 0.0603 | 0.0614 | 0.0621 | 0.0626 | 0.0629 | 0.0639 | 0.0649 |
| 0.8 | 0.0549 | 0.0567 | 0.0593 | 0.0609 | 0.0620 | 0.0628 | 0.0649 | 0.0672 |
| 0.7 | 0.0509 | 0.0541 | 0.0585 | 0.0613 | 0.0633 | 0.0648 | 0.0684 | 0.0725 |
| 0.6 | 0.0475 | 0.0525 | 0.0599 | 0.0648 | 0.0681 | 0.0705 | 0.0767 | 0.0831 |
| 0.5 | 0.0448 | 0.0529 | 0.0658 | 0.0743 | 0.0800 | 0.0841 | 0.0936 | 0.1032 |
| 0.4 | 0.0432 | 0.0575 | 0.0827 | 0.0975 | 0.1066 | 0.1127 | 0.1267 | 0.1401 |
| 0.3 | 0.0437 | 0.0767 | 0.1253 | 0.1490 | 0.1632 | 0.1726 | 0.1941 | 0.2148 |
| 0.2 | 0.0529 | 0.1454 | 0.2401 | 0.2857 | 0.3128 | 0.3309 | 0.3721 | 0.4117 |
| 0.1 | 0.1597 | 0.4887 | 0.8071 | 0.9604 | 1.0515 | 1.1121 | 1.2508 | 1.3838 |
| 0 | 0.0161 | 0.0161 | 0.0161 | 0.0161 | 0.0161 | 0.0161 | 0.0161 | 0.0161 |

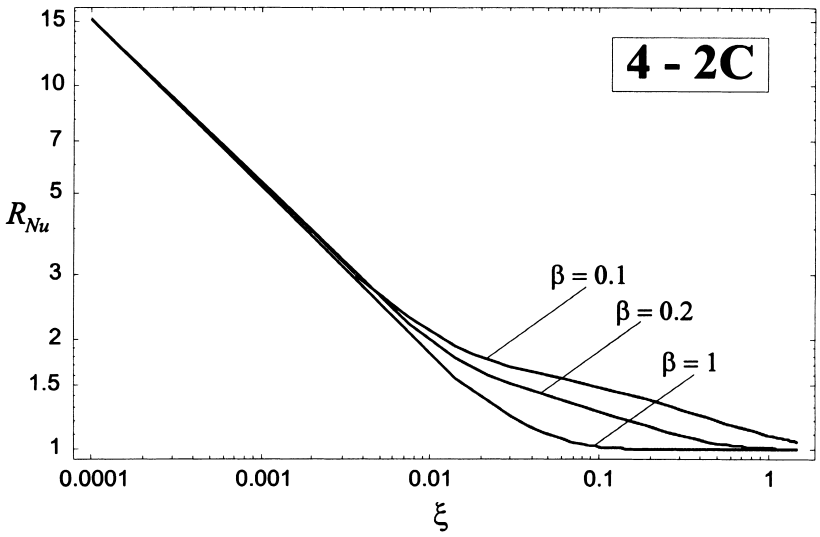


Fig. 2. Plots of $R_{Nu}$ vs. $\xi$ for the boundary condition 4 or 2C. The plots refer to three different values of $\beta$ and to any value of $Br$.

in the cases 4, 3L, 3S, 2L, 2S, 2C, 1L and 1S. The values of $L^*_{th}$ reported in this table for $\beta \to 0$ are all coincident except in the cases 1S and 2S where, in the absence of viscous dissipation, $Nu$ is undefined. As expected, the columns which refer to cases 4 and 2C coincide. Also the columns which refer to cases 2L and 1L are coincident, as well as those for the cases 2S and 1S. The dependence of $L^*_{th}$ on $\beta$ is different in the eight cases. More precisely, for the cases 4, 3S, 2S, 2C and 1S, $L^*_{th}$ is a monotonically decreasing function of $\beta$. For the cases 2L and 1L, $L^*_{th}$ is a monotonically increasing function of $\beta$. Finally, in the case 3L, $L^*_{th}$ has a non-monotonic dependence on $\beta$ in the range $0.7 < \beta < 1$. As it has been already pointed out, Gao–Hartnett's definition of local Nusselt number [6] also adopted by Spiga and Morini [8] agrees with Eq. (38) in the case 4. However, even in this case, the values of $L^*_{th}$ reported in Table 3 are not in good agreement with those obtained by Spiga and Morini [8], the discrepancies being of about 10%. In the authors' opinion, these discrepancies should be caused by a lower accuracy in the numerical evaluation of $L^*_{th}$ performed in Ref. [8]. As is easily inferred from Table 3, with the exception of the cases 2L and 1L, the limit $\beta \to 0$ of $L^*_{th}$ evaluated by Eq. (52) is ill-defined. Indeed, the value of $L^*_{th}$ for $\beta = 0$ reported in Table 3 is obtained by employing Eq. (54).

In Table 4, values of $L^*_{th}$ in the case 2L are reported for some values of $\beta$ and $Br$. This table shows that, for a fixed value of $\beta$, $L^*_{th}$ is a monotonic increasing function of $Br$, with the exception of the cases $\beta = 1$ and $\beta = 0$ where $L^*_{th}$ is independent of $Br$. On the other hand, the dependence of $L^*_{th}$ on $\beta$ is non-monotonic. The values reported in Table 4 reveal, for a fixed $Br$, the existence of an aspect ratio which yields a minimum $L^*_{th}$. This aspect ratio increases with $Br$ and approaches $\beta = 1$ for $Br \to \infty$. The values of $L^*_{th}$ in the limiting case of adiabatic walls ($Br \to \infty$) are not reported in Table 4 since, as is easily inferred from Eq. (52), these values coincide with those for the case 4, already reported in Table 3. On account of the values reported in Table 4, one can conclude that the effect of viscous dissipation on $L^*_{th}$ is more and more apparent as $\beta$ decreases from 1 to 0.1. Moreover, it should be pointed out that Table 4 reveals a behavior in the limit $\beta \to 0$ different from that in the case $Br = 0$. More precisely, in the latter case, the limit for $\beta \to 0$ of $L^*_{th}$ for the boundary condition 2L is well defined, as is shown in Table 3. On the contrary, this limit is ill-defined for $Br \neq 0$, as it can be inferred from Eq. (52). A comparison between Tables 3 and 4 shows that the column for the case 3L in Table 3 coincides with the column for $Br = 1$ in Table 4. This is not surprising since, as it is easily proved by employing Eq. (52), $R_{Nu}$ evaluated for $Br = 0$ and the boundary condition 3L coincides with $R_{Nu}$ evaluated for $Br = 1$ and the boundary condition 2L.

The behavior of $R_{Nu}$ in the thermal entrance region is represented in Figs. 2 and 3. As it has been pointed out above, the boundary conditions 4 and 2C yield the same $R_{Nu}$, which is independent of $Br$. Fig. 2 refers to the boundary conditions 4 and 2C. In this figure, plots of $R_{Nu}$ versus $\xi$ are reported for $\beta = 1$, $\beta = 0.2$ and $\beta = 0.1$. In agreement with the values of the dimensionless thermal entrance length given in Table 3, Fig. 2 reveals that the dependence of $R_{Nu}$ on $\beta$ is stronger for low values of the aspect ratio and that $L^*_{th}$ undergoes a rapid increase for small $\beta$. Fig. 3 refers to the

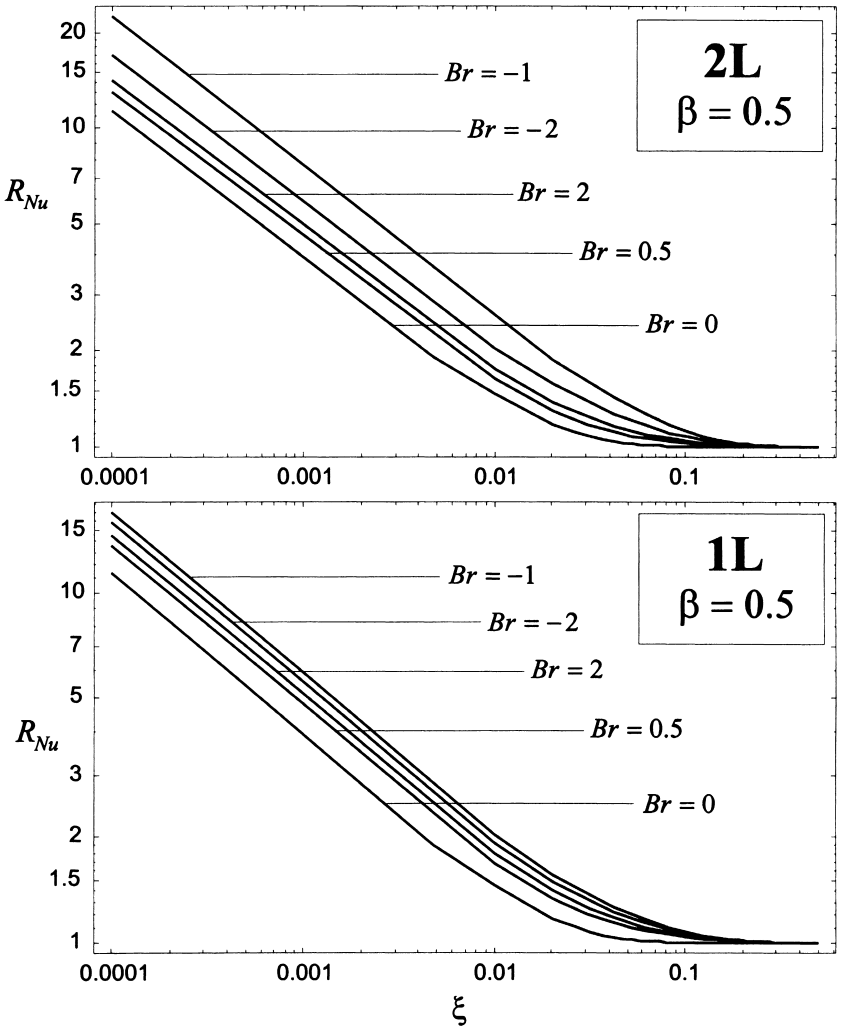


Fig. 3. Plots of $R_{Nu}$ vs. $\xi$ for the boundary condition 2L and for the boundary condition 1L. The plots refer to $\beta = 0.5$ and to different values of $Br$.

aspect ratio $\beta = 0.5$ and displays a comparison between the behavior of $R_{Nu}$ in the case 2L and in the case 1L. In each case, plots are reported for different values of $Br$. The difference between the cases 2L and 1L is more apparent for $Br < 0$. In fact, as it has been pointed above, for $Br = 0$, the boundary conditions 2L and 1L yield the same values of $R_{Nu}$. Moreover, the effect of viscous dissipation is more important for $Br < 0$ since, as is easily checked by employing Table 2, $Nu_\infty$ is singular for $Br = -1/2$ in the case 2L, while it is singular for $Br = -1/4$ in the case 1L. When $Nu_\infty$ is singular, $R_{Nu}$ is identically vanishing for every value of $\xi$.

Fig. 4 refers to $\beta = 1$, $Br = 1$ and to the boundary condition 4. In this figure, plots of the distributions of $\Delta\theta = \theta - \theta_b$ at different duct sections which correspond to $\xi = 0.001$, $\xi = 0.005$, $\xi = 0.02$ and $\xi = 0.1$ are reported. Fig. 4 is a representation of the thermal boundary layer development. For $\xi = 0.001$, the fluid is almost isothermal and a steep temperature change occurs in the neighborhood of the duct walls. For higher values of $\xi$, the temperature gradient at the duct walls becomes smaller. For $\xi = 0.1$, $\Delta\theta$ has almost reached its fully developed distribution. Fig. 4 shows that, at each channel section, the highest values of $\theta$ occur at the four edges of the duct.

## 5. Exponential axial change of the wall heat flux

In this section, the case of a peripherally uniform wall heat flux which undergoes an exponential axial

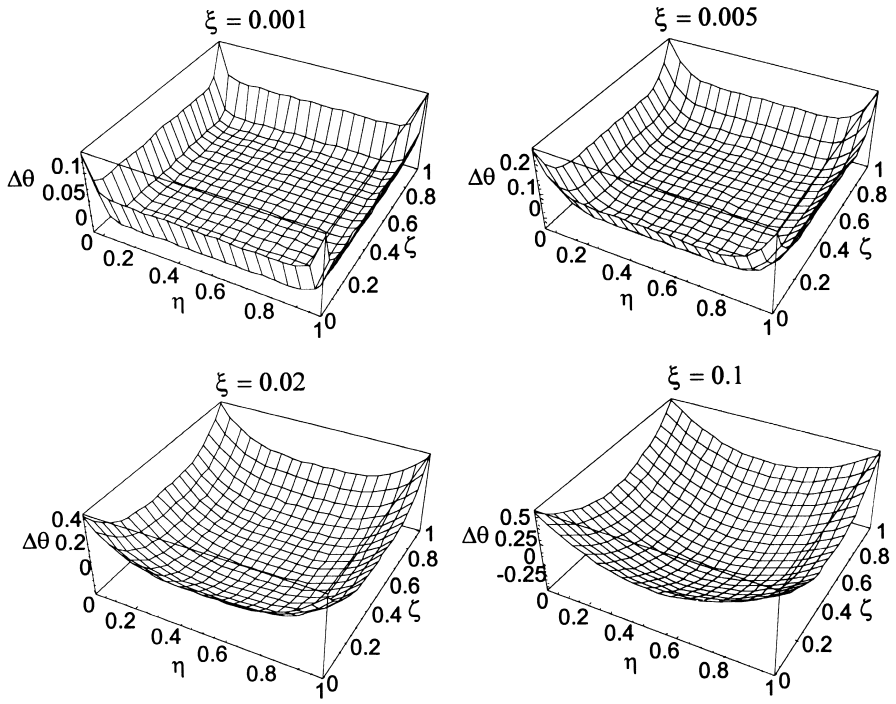


Fig. 4. Plots of $\Delta\theta = \theta - \theta_b$ for the boundary condition 4 with $\beta = 1$ and $Br = 1$. The plots refer to different values of $\xi$.

change is analyzed by employing the expressions of the dimensionless temperature and of the local Nusselt number obtained in Sections 2 and 3.

Let us assume that the functions $g_1(\xi)$, $g_2(\xi)$, $g_3(\xi)$ and $g_4(\xi)$ are given by

$$g_1(\xi) = g_2(\xi) = g_3(\xi) = g_4(\xi) = U(\xi)e^{2a\xi}, \tag{55}$$

where $a$ is an arbitrary real number.

On account of Eq. (55), Eqs. (30) and (31) yield

$$\theta_1(\xi,\eta) = \frac{Br+1}{\gamma}\left[H\left(\xi\gamma^2,\eta\right) + H\left(\xi\gamma^2,1-\eta\right)\right] + \frac{2a}{\gamma}\left[M\left(\xi,\gamma^2,\eta\right) + M\left(\xi,\gamma^2,1-\eta\right)\right], \tag{56}$$

$$\theta_2(\xi,\zeta) = \frac{(Br+1)\beta}{\gamma}\left[H\left(\frac{\xi\gamma^2}{\beta^2},\frac{\zeta}{\beta}\right) + H\left(\frac{\xi\gamma^2}{\beta^2},1-\frac{\zeta}{\beta}\right)\right] + \frac{2a\beta}{\gamma}\left[M\left(\xi,\frac{\gamma^2}{\beta^2},\frac{\zeta}{\beta}\right) + M\left(\xi,\frac{\gamma^2}{\beta^2},1-\frac{\zeta}{\beta}\right)\right], \tag{57}$$

where function $M(\xi,p,\omega)$ is defined as

$$M(\xi,p,\omega) = \int_0^\xi e^{2a\xi'} H\left(p\left(\xi-\xi'\right),\omega\right) d\xi'. \tag{58}$$

On account of Eq. (25), Eq. (58) can be rewritten in the form

$$M(\xi,p,\omega) = \frac{p}{4a^2}\left(e^{2a\xi} - 2a\xi - 1\right) + \frac{1-3\omega^2}{12a}\left(1-e^{2a\xi}\right) - \frac{2e^{2a\xi}}{\pi^2}\sum_{n=1}^{\infty}\frac{(-1)^n}{n^2\left(2a+n^2\pi^2p\right)}\cos(n\pi\omega) + \frac{2}{\pi^2}\sum_{n=1}^{\infty}\frac{(-1)^n}{n^2\left(2a+n^2\pi^2p\right)}\cos(n\pi\omega)\exp\left(-n^2\pi^2p\xi\right). \tag{59}$$

By employing the Fourier series method [16], it is easily verified that the identities

$$\sum_{n=1}^{\infty}\frac{(-1)^n}{2a+n^2\pi^2p}\cos(n\pi\omega) = \frac{\cosh\left(\omega\sqrt{2a/p}\right)}{2\sqrt{2ap}\,\sinh\left(\sqrt{2a/p}\right)} - \frac{1}{4a}, \tag{60}$$

$$\sum_{n=1}^{\infty}\frac{(-1)^n}{n^2}\cos(n\pi\omega) = \frac{\pi^2}{12}\left(3\omega^2-1\right), \tag{61}$$

hold. As a consequence of Eqs. (60) and (61), one obtains

$$\begin{aligned}\sum_{n=1}^{\infty}\frac{(-1)^n}{n^2\left(2a+n^2\pi^2p\right)}\cos(n\pi\omega)&=\frac{1}{2a}\sum_{n=1}^{\infty}\frac{(-1)^n}{n^2}\cos(n\pi\omega)\\&-\frac{\pi^2p}{2a}\sum_{n=1}^{\infty}\frac{(-1)^n}{2a+n^2\pi^2p}\cos(n\pi\omega)\\&=\frac{\pi^2p}{8a^2}+\frac{\pi^2}{24a}(3\omega^2-1)-\frac{\pi^2}{4a}\sqrt{\frac{p}{2a}}\frac{\cosh\left(\omega\sqrt{2a/p}\right)}{\sinh\left(\sqrt{2a/p}\right)}.\end{aligned}\tag{62}$$

By employing Eq. (62), Eq. (59) can be rewritten as

$$\begin{aligned}M(\xi,p,\omega)&=-\frac{p}{4a^2}(2a\xi+1)+\frac{1-3\omega^2}{12a}\\&+\frac{1}{2a}\sqrt{\frac{p}{2a}}\frac{\cosh\left(\omega\sqrt{2a/p}\right)}{\sinh\left(\sqrt{2a/p}\right)}\mathrm{e}^{2a\xi}\\&+\frac{2}{\pi^2}\sum_{n=1}^{\infty}\frac{(-1)^n}{n^2\left(2a+n^2\pi^2p\right)}\cos(n\pi\omega)\exp\left(-n^2\pi^2p\xi\right).\end{aligned}\tag{63}$$

On account of Eq. (55), Eqs. (36) and (37) yield

$$\theta_{1b}(\xi)=2\gamma Br\xi+\frac{\gamma}{a}(\mathrm{e}^{2a\xi}-1),$$

$$\theta_{2b}(\xi)=2\frac{\gamma}{\beta}Br\xi+\frac{\gamma}{\beta a}(\mathrm{e}^{2a\xi}-1).\tag{64}$$

As a consequence of Eqs. (43) and (55), for $\xi>0$, the local Nusselt number is given by

$$Nu=\frac{\mathrm{e}^{2a\xi}}{\theta_{w,m}(\xi)-\theta_b(\xi)}.\tag{65}$$

Eqs. (25), (42), (56), (57), (63) and (64) imply that the difference $\theta_{w,m}(\xi)-\theta_b(\xi)$ can be expressed as

$$\begin{aligned}\theta_{w,m}(\xi)-\theta_b(\xi)&=\frac{Br}{6}\\&+\mathrm{e}^{2a\xi}\left[\frac{\gamma}{2\beta\sqrt{2a}}\coth\left(\frac{\beta\sqrt{2a}}{2\gamma}\right)\right.\\&\left.+\frac{\gamma}{2\sqrt{2a}}\coth\left(\frac{\sqrt{2a}}{2\gamma}\right)-\frac{2\left(\beta^2+1\right)}{a(\beta+1)^2}\right]\\&-\frac{1}{2\pi^2}\sum_{n=1}^{\infty}\frac{(Br+1)\left(a+2n^2\pi^2\gamma^2\right)-a}{n^2\left(a+2n^2\pi^2\gamma^2\right)}\\&\times\exp\left(-4n^2\pi^2\gamma^2\xi\right)\\&-\frac{1}{2\pi^2}\sum_{n=1}^{\infty}\frac{(Br+1)\left(a+2n^2\pi^2\gamma^2/\beta^2\right)-a}{n^2\left(a+2n^2\pi^2\gamma^2/\beta^2\right)}\\&\times\exp\left(-4n^2\pi^2\frac{\gamma^2}{\beta^2}\xi\right).\end{aligned}\tag{66}$$

If $a>0$, Eqs. (65) and (66) predict the existence of a fully developed Nusselt number in the limit $\xi\to\infty$. The fully developed value $Nu_\infty$ is given by

$$Nu_\infty=\frac{1}{\frac{\gamma}{2\beta\sqrt{2a}}\coth\left(\frac{\beta\sqrt{2a}}{2\gamma}\right)+\frac{\gamma}{2\sqrt{2a}}\coth\left(\frac{\sqrt{2a}}{2\gamma}\right)-\frac{2\left(\beta^2+1\right)}{a(\beta+1)^2}}.\tag{67}$$

As expected, for $a>0$, the fully developed value of $Nu$ is independent of $Br$. Indeed, an exponential axial increase of the wall heat flux implies that, sufficiently far from the inlet section, the effect of viscous dissipation becomes negligible, whatever the value of $Br$ may be. On account of Eqs. (65) and (66), for $a<0$ and for any non-vanishing value of $Br$, the limit $\xi\to\infty$ of $Nu$ is zero. On the other hand, Eqs. (65) and (66) imply that, for $Br=0$, the limit $\xi\to\infty$ of $Nu$ is zero only if $a<-2\pi^2\gamma^2$, while, if $-2\pi^2\gamma^2<a<0$, a fully developed value of $Nu$ is reached and can be expressed as

$$Nu_\infty=\frac{1}{\frac{2\left(\beta^2+1\right)}{|a|(\beta+1)^2}-\frac{\gamma}{2\beta\sqrt{2|a|}}\cot\left(\frac{\beta\sqrt{2|a|}}{2\gamma}\right)-\frac{\gamma}{2\sqrt{2|a|}}\cot\left(\frac{\sqrt{2|a|}}{2\gamma}\right)}.$$

Obviously, the fully developed values of $Nu$ evaluated by Eq. (68) have no physical interest. In fact, in some cases, the Brinkman number can be very small and even exceptionally small, but in no case it can be exactly zero. As a consequence, one can conclude that, in every practical case with $a<0$, the limit $\xi\to\infty$ of $Nu$ is zero. It should be pointed out that the behavior of $Nu$ in the fully developed region for exponential

Table 5
Values of $Nu_\infty$ for an exponentially varying wall heat flux

| $a$ | $\beta = 1$ | $\beta = 0.8$ | $\beta = 0.6$ | $\beta = 0.4$ | $\beta = 0.2$ | $\beta = 0.1$ | $\beta \to 0$ | Circular duct [11] |
|---|---|---|---|---|---|---|---|---|
| 0 | 6.0000 | 6.0000 | 6.0000 | 6.0000 | 6.0000 | 6.0000 | 12.000 | 8.0000 |
| 1 | 6.1972 | 6.2041 | 6.2349 | 6.3329 | 6.7530 | 7.6739 | 12.100 | 8.1650 |
| 10 | 7.7655 | 7.8004 | 7.9477 | 8.3412 | 9.3898 | 10.564 | 12.966 | 9.5176 |
| 20 | 9.2012 | 9.2417 | 9.4094 | 9.8364 | 10.875 | 11.934 | 13.871 | 10.809 |
| 30 | 10.430 | 10.470 | 10.637 | 11.054 | 12.043 | 13.019 | 14.724 | 11.945 |
| 40 | 11.516 | 11.556 | 11.716 | 12.119 | 13.061 | 13.974 | 15.531 | 12.967 |
| 50 | 12.499 | 12.536 | 12.692 | 13.079 | 13.981 | 14.846 | 16.298 | 13.902 |
| 60 | 13.401 | 13.437 | 13.588 | 13.963 | 14.831 | 15.658 | 17.030 | 14.768 |
| 70 | 14.239 | 14.274 | 14.421 | 14.785 | 15.626 | 16.421 | 17.730 | 15.577 |
| 80 | 15.025 | 15.059 | 15.202 | 15.558 | 16.375 | 17.145 | 18.402 | 16.340 |
| 90 | 15.767 | 15.801 | 15.941 | 16.289 | 17.086 | 17.835 | 19.049 | 17.062 |
| 100 | 16.472 | 16.505 | 16.643 | 16.984 | 17.765 | 18.494 | 19.673 | 17.751 |
| 500 | 33.758 | 33.786 | 33.901 | 34.182 | 34.802 | 35.356 | 36.202 | 34.875 |
| 1000 | 46.815 | 46.842 | 46.952 | 47.221 | 47.810 | 48.330 | 49.114 | 47.897 |
| 5000 | 102.04 | 102.07 | 102.17 | 102.43 | 102.97 | 103.45 | 104.17 | 103.08 |
| 10,000 | 143.45 | 143.48 | 143.58 | 143.83 | 144.37 | 144.84 | 145.54 | 144.48 |
| 50,000 | 318.24 | 318.27 | 318.37 | 318.61 | 319.14 | 319.60 | 320.28 | 319.25 |
| 100,000 | 449.22 | 449.25 | 449.35 | 449.59 | 450.12 | 450.58 | 451.25 | 450.23 |

wall heat flux is analogous to that analyzed in the case of circular ducts [12].

It is easily verified that, in the limit $\beta \to 0$, i.e., for a plane parallel channel, Eq. (66) yields

$$\theta_{w,m}(\xi) - \theta_b(\xi) = \frac{Br}{12} + e^{2a\xi}\left[\frac{1}{\sqrt{2a}}\coth\left(\frac{1}{2}\sqrt{\frac{a}{2}}\right) - \frac{2}{a}\right] - \frac{1}{2\pi^2}\sum_{n=1}^{\infty}\frac{(Br+1)(a+8n^2\pi^2) - a}{n^2(a+8n^2\pi^2)}\exp(-16n^2\pi^2\xi). \tag{69}$$

As a consequence of Eqs. (65) and (69), if $a > 0$ and $\beta \to 0$, the fully developed value of $Nu$ is given by

$$Nu_\infty = \frac{a\sqrt{2a}}{a\coth\left(\frac{1}{2}\sqrt{\frac{a}{2}}\right) - 2\sqrt{2a}}. \tag{70}$$

The right-hand side of Eq. (70) can be also obtained by taking the limit $\beta \to 0$ of the right-hand side of Eq. (67). Obviously, if $a < 0$ and $Br \neq 0$, Eqs. (65) and (69) imply that the limit $\xi \to \infty$ of $Nu$ is zero.

In Table 5, values of $Nu_\infty$ for different aspect ratios and for different values of $a$ are compared with the values of $Nu_\infty$ evaluated in Ref. [11] in the case of slug-flow forced convection in a circular duct with an exponentially varying wall heat flux. The comparison reveals that, for any fixed $a$, the value of $Nu_\infty$ for a circular duct lies between the value for a square duct ($\beta = 1$) and the value for a parallel plate channel ($\beta \to 0$). Moreover, the discrepancies between the value of $Nu_\infty$ for a square duct, the value for a parallel plate channel and the value for a circular duct tend to become negligible as $a$ increases. In Table 5, the values of $Nu_\infty$ in the limit $\beta \to 0$ are evaluated by employing Eq. (70), while the values in the limit $a \to 0$ are obtained by evaluating the limit either of the right-hand side of Eq. (67) or of the right-hand side of Eq. (70). It can be pointed out that, for a fixed $a > 0$, the value of $Nu_\infty$ is a decreasing function of $\beta$ and that, for a fixed $\beta$, the value of $Nu_\infty$ is an increasing function of $a$.

In Fig. 5, plots of $R_{Nu}$ versus $\xi$ are reported for $\beta = 1$, $a = 10$ and for different values of $Br$. This figure shows that, for positive values of $Br$, $R_{Nu}$ initially decreases in the thermal entrance region, reaches a minimum and increases to its asymptotic value 1. The behavior for $Br = 0$, $Br = -0.5$ and $Br = -1$ is different, since $R_{Nu}$ is a monotonic decreasing function of $\xi$ which tends asymptotically to 1. Finally, the plot for $Br = -10$ displays a singularity of $R_{Nu}$ for $\xi = 0.1278$. This singularity occurs because, for $Br = -10$, $a = 10$ and $\xi = 0.1278$, the dimensionless wall temperature $\theta_{w,m}$ coincides with the dimensionless bulk temperature $\theta_b$. Indeed, an analysis of the data for $a = 10$ and $\beta = 1$ reveals that, for every value of $Br$ such that $Br < -1$, there exists a value of $\xi$ greater than zero which yields a singularity of $R_{Nu}$ and, hence, of $Nu$. However, this

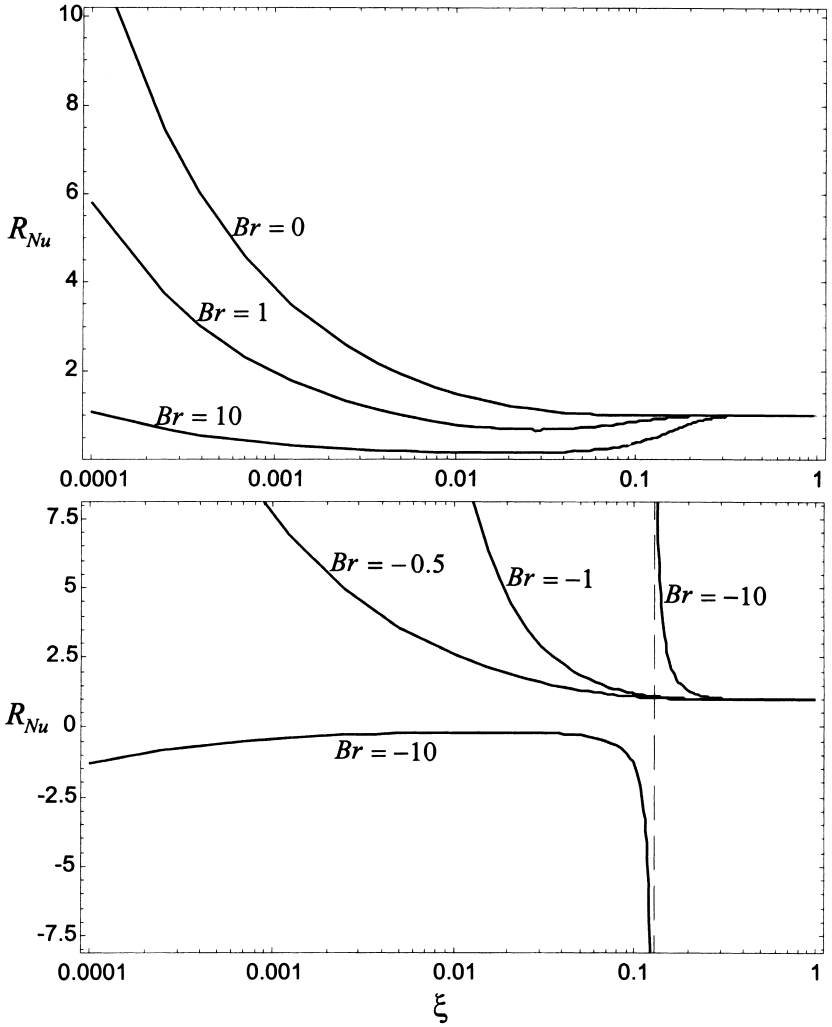


Fig. 5. Plots of $R_{Nu}$ vs. $\xi$ for an exponentially varying wall heat flux with $a = 10$. The plots refer to $\beta = 1$ (square duct) and to different values of $Br$.

value of $\xi$ is a decreasing function of $Br$ in the range $Br < -1$ and tends to zero in the limit $Br \to -1$. A quite similar behavior has been observed also in the thermal entrance region of circular ducts for slug-flow forced convection with an exponentially varying wall heat flux [12].

## 6. Conclusions

The stationary forced convection in a rectangular duct with prescribed heat fluxes on the four walls has been investigated in the case of slug flow, by taking into account the effect of viscous dissipation. An analytical solution of the energy balance equation has been found for arbitrary axially varying heat fluxes prescribed on the four duct walls. The solution has been obtained by employing a superposition method and the Laplace transform technique. Detailed analyses have been performed both for the eight boundary conditions 4, 3L, 3S, 2L, 2S, 2C, 1L and 1S proposed by Gao and Hartnett [6] and for a peripherally uniform wall heat flux which undergoes an exponential axial variation.

The most important results obtained in the preceding sections are the following. The Brinkman number affects the ratio $R_{Nu} = Nu/Nu_\infty$ and, as a consequence, the value of the dimensionless thermal entrance length

in the cases 3L, 3S, 2L, 2S, 1L and 1S, but not in the cases 4 and 2C. For a square duct ($\beta = 1$), at every dimensionless axial position $\xi$, the ratio $R_{Nu}$ is the same for all the eight Gao–Hartnett's boundary conditions and is independent of the Brinkman number, $Br$. Moreover, a non-vanishing value of $Br$ implies that, in the limit $\beta \to 0$, $Nu_\infty$ and $L^*_{\rm th}$ for a rectangular duct do not coincide with those for a plane parallel channel, even for the boundary conditions 2L and 1L. In the case of a peripherally uniform wall heat flux which undergoes an exponential axial variation, it has been shown that, for positive values of the parameter $a$, the fully developed Nusselt number is independent of $Br$. However, if $a > 0$ and $Br < -1$, in the thermal entrance region there exists an axial position where the local Nusselt number becomes singular. The effect of viscous dissipation may be very important for exponentially decreasing wall heat fluxes ($a < 0$). In this case, for any non-vanishing value of $Br$, the local Nusselt number tends to zero in the limit $\xi \to \infty$.

## Appendix

Let us evaluate the inverse Laplace transform which appears at the right-hand side of Eq. (24). Function $\tilde{H}(s,\omega)$ has no branch points, has a double pole for $s = 0$ and has an infinite sequence of simple poles for $s = s_n$, where, for every positive integer $n$, $s_n = -n^2\pi^2$. The classical procedure for the inversion of Laplace transforms consists of the following steps (see Ref. [14] for details). The Laplace inversion integral is expressed as a contour integral in the complex plane along the Bromwich contour closed by an arc of circle. Then, the integral is evaluated by using the Cauchy residue theorem. By means of this procedure, one obtains

$$H(t,\omega) = \mathrm{Res}\left[\frac{\mathrm{e}^{st}\cosh\left(\omega\sqrt{s}\right)}{s\sqrt{s}\sinh\left(\sqrt{s}\right)};s=0\right] + \sum_{n=1}^{\infty}\mathrm{Res}\left[\frac{\mathrm{e}^{st}\cosh\left(\omega\sqrt{s}\right)}{s\sqrt{s}\sinh\left(\sqrt{s}\right)};s=s_n\right]. \tag{A1}$$

The residue at $s = 0$ is given by

$$\mathrm{Res}\left[\frac{\mathrm{e}^{st}\cosh\left(\omega\sqrt{s}\right)}{s\sqrt{s}\sinh\left(\sqrt{s}\right)};s=0\right] = \left\{\frac{\mathrm{d}}{\mathrm{d}s}\left[\frac{\mathrm{e}^{st}\sqrt{s}\cosh\left(\omega\sqrt{s}\right)}{\sinh\left(\sqrt{s}\right)}\right]\right\}_{s=0} = t + \frac{\omega^2}{2} - \frac{1}{6}, \tag{A2}$$

while, for every $n \geq 1$, the residue in $s = s_n$ can be expressed as

$$\mathrm{Res}\left[\frac{\mathrm{e}^{st}\cosh\left(\omega\sqrt{s}\right)}{s\sqrt{s}\sinh\left(\sqrt{s}\right)};s=s_n\right] = \frac{\exp\left(-n^2\pi^2 t\right)\cos(n\pi\omega)}{\left\{\frac{\mathrm{d}}{\mathrm{d}s}\left[s\sqrt{s}\sinh\left(\sqrt{s}\right)\right]\right\}_{s=s_n}} = -\frac{2(-1)^n}{n^2\pi^2}\exp\left(-n^2\pi^2 t\right)\cos(n\pi\omega). \tag{A3}$$

Eqs. (A1)–(A3) yield Eq. (25).

## References


[1] R.K. Shah, A.L. London, Laminar flow forced convection in ducts, Advances in Heat Transfer (suppl. 1), Academic Press, New York, 1978.

[2] R.K. Shah, M.S. Bhatti, Laminar convective heat transfer in ducts, in: S. Kakaç, R.K. Shah, W. Aung (Eds.), Handbook of Single-Phase Convective Heat Transfer, Wiley, New York, 1987 (chapter 3).

[3] J.P. Hartnett, M. Kostic, Heat transfer to Newtonian and non-Newtonian fluids in rectangular ducts, Advances in Heat Transfer 19 (1989) 247–356.

[4] J.B. Aparecido, R.M. Cotta, Thermally developing laminar flow inside rectangular ducts, International Journal of Heat and Mass Transfer 33 (1990) 341–347.

[5] S.X. Gao, J.P. Hartnett, Non-Newtonian fluid laminar flow and forced convection heat transfer in rectangular ducts, International Communications in Heat and Mass Transfer 19 (1992) 673–686.

[6] S.X. Gao, J.P. Hartnett, Analytical Nusselt number predictions for slug flow in rectangular duct, International Communications in Heat and Mass Transfer 20 (1993) 751–760.

[7] B.T.F. Chung, Z.J. Zhang, G. Li, Thermally developing convection from Newtonian flow in rectangular ducts with uniform heating, Journal of Thermophysics and Heat Transfer 7 (1993) 534–536.

[8] M. Spiga, G.L. Morini, The thermal entrance length problem for slug flow in rectangular ducts, ASME Journal of Heat Transfer 118 (1996) 979–982.

[9] M. Spiga, G.L. Morini, The developing Nusselt numbers for slug flow in rectangular ducts, International Journal of Heat and Mass Transfer 41 (1998) 2799–2807.

[10] G.L. Morini, M. Spiga, P. Tartarini, Laminar viscous dissipation in rectangular ducts, International Communications in Heat and Mass Transfer 25 (1998) 551–560.

[11] A. Barletta, On forced convection in a circular duct with slug flow and viscous dissipation, International Communications in Heat and Mass Transfer 23 (1996) 69–78.

[12] A. Barletta, E. Zanchini, Forced convection in the thermal entrance region of a circular duct with slug flow and viscous dissipation, International Journal of Heat and Mass Transfer 40 (1997) 1181–1190.

[13] A. Barletta, Slug flow heat transfer in circular ducts with viscous dissipation and convective boundary conditions, International Journal of Heat and Mass Transfer 40 (1997) 4219–4228.
[14] L. Debnath, Integral Transforms and their Applications, 1st ed, CRC Press, New York, 1995.
[15] R.K. Shah, Laminar flow friction and forced convection heat transfer in ducts of arbitrary geometry, International Journal of Heat and Mass Transfer 18 (1975) 849–862.
[16] M.R. Spiegel, Fourier Analysis, McGraw-Hill, New York, 1974.